

DNS ASSISTED MODELING OF BUBBLY FLOWS IN VERTICAL CHANNELS

G. Tryggvason, M. Ma and J. Lu

University of Notre Dame

Department of Aerospace and Mechanical Engineering

Notre Dame, IN 46556, USA

gtryggva@nd.edu; Ming.Ma.28@nd.edu; jlu2@nd.edu

ABSTRACT

The transient motion of bubbly flows, in vertical channels, is studied, using direct numerical simulations (DNS), where every continuum length- and time-scale are resolved. A simulation of a large number of bubbles of different sizes at a friction Reynolds number of 500 shows that small bubbles quickly migrate to the wall, but the bulk flow takes much longer to adjust to the new bubble distribution. Simulations of much smaller laminar systems with several spherical bubbles have been used to examine the full transient motion and those show a non-monotonic evolution where all the bubbles first move toward the walls and then the liquid slowly slows down, eventually allowing some bubbles to return to the center of the channel. Unlike the statistically steady state, where the flow structure is relatively simple and in some cases depends only on the sign of the bubble lift coefficient, the transient evolution is more sensitive to the governing parameters. Early efforts to use DNS results to provide values for the unresolved closure terms in a simple average model for the flow, found by statistical learning from the data, using neural networks is discussed. The prospects of using the results from simulations of large system with bubbles of different sizes in turbulent flows for LES-like simulations are explored, including the simplification of the interface structure by filtering. Finally, preliminary results for flows undergoing topology changes are shown.

KEYWORDS

DNS, bubbly flows, statistical learning, two-fluid model, turbulence

1. INTRODUCTION

Direct numerical simulations (DNS) of multiphase flow, where every continuum time- and length-scale are fully resolved, have over the last two decades provided significant insight into the dynamics of such flows. For most industrial and natural systems, however, DNS require too fine grid resolution to be practical. Furthermore, since the small-scale behavior often exhibits considerable universality, it is likely that in many cases the small scales can be modeled, rather than fully resolved. For single-phase flows, DNS have already helped significantly with the modeling of unresolved scales, including how they depend on the large scale resolved flow and how the small scales in turn influence the larger scales.

Modeling of multiphase flows generally builds on the two-fluid approach, where separate equations are solved for the average motion of the different fluids. For recent reviews see [1], for example. Although DNS of multiphase flows have progressed rapidly during the last two decades, attempts to use DNS results to help modeling of multiphase flows are still rare. Here, we review briefly simulations of bubbly

flows in vertical channels, the insight such simulations have provided, and how the results may help the development of closure terms for equations for the average, or the large-scale, flow.

2. COMPUTATIONAL SETUP

The simulations are done using a finite-volume/front tracking method originally introduced in [2]. The Navier-Stokes equations are solved using the “one-fluid” formulation where a single set of equations is discretized on a regular structured grid covering the entire computational domain. The equations govern the motion of all the fluids involved, and the different constituents are identified by the differences in their material properties. Surface tension is added as a smoothed body force at the interface separating the different fluids. This formulation is the foundation for most other methods that have been used for DNS of multiphase flows, such as VOF and level-set methods. To identify the different fluids a marker function is usually advected directly on the fluid grid. In the front-tracking method, on the other hand, we advect the interface itself. The interface is represented by connected marker points that are moved with the fluid velocity, interpolated from the fixed fluid grid. Once the marker points have been advected, a marker function is constructed from the new interface location. The front is also used to compute surface tension, which is then smoothed on to the fluid grid and added to the discrete Navier-Stokes equations. In addition to the computation of the surface tension and the construction of the marker function, the chief challenge in front-tracking is the dynamic updating of the front, whereby marker points are added or deleted to maintain the point density needed to fully resolve the interface. For a detailed description of the original method, as well as various improvements and refinements, and validation and accuracy tests, see [2-5].

For the computations presented here, the domain is a rectangular channel where the left and right boundaries are rigid no-slip walls and periodic boundary conditions are applied in the streamwise and spanwise direction. The flow is driven upward by an imposed pressure gradient, yielding the desired friction Reynolds number.

3. SMALL SYSTEMS

Bubbly flows in vertical channels are a natural starting point for attempts to use DNS data to model the average flow. The flow is homogeneous in the streamwise and the spanwise direction and the average motion depends only on the wall-normal coordinate. Furthermore, if the channel is completely vertical, the average motion should be symmetric around the center plane. This allows the DNS data to be averaged over not only the streamwise and the spanwise direction but also over the left and right side of the channel.

3.1 Steady-State and Transient Evolution

Two-dimensional laminar bubbly flows in vertical channels were examined in [6] and the averaged DNS solution at (statistically) steady state compared with predictions by an analytical model developed in reference [7]. It was found that the model predicted the void fraction profile well for both upflow and downflow. The velocity profile was also well-predicted for downflow but for upflow the model over-predicted the velocity. However, once the coefficients had been adjusted for one case, the model did a reasonable job of predicting the velocity for other operating parameters. Subsequent investigations, in [8], showed that the overall flow had a very simple structure, consisting of a nearly homogeneous core region and thin wall-layers. The structure is determined by the lift forces on the bubbles, which drive them toward the side where the liquid velocity is largest, in a frame of reference moving with the bubble. Thus, in upflow the bubbles are driven toward the walls. Studies of the magnitude of the lift force and how it depends on the shear and other properties of the flow include [9-12]. The lift force depends strongly on the deformability of the bubble and larger bubbles (more deformable) tend to have either little lift or a lift in the opposite direction from the nearly spherical ones [13]. Very little is known about the lift on many

bubbles in high void fraction flows, although preliminary studies can be found in [14]. The vertical migration of bubbles from the core, to the walls, increases the average density of the mixture in the core and if there are enough bubbles the weight of the mixture eventually balances the imposed pressure gradient and as the shear becomes zero the migration of bubbles stops. The void fractions in the core and the wall-layer are therefore easily predicted. One of the main conclusions of these studies is that the steady state flow does not depend on the magnitude of the lift coefficient—only its sign. This suggests that if we intend to use the DNS results to evaluate and help construct models of the average flow, it is necessary to examine the transient motion.

Recently, DNS have been used to examine the transient evolution of both laminar and turbulent channel flows, leading to considerable increase of the understanding of such flows. The transient evolution is important for several reasons. First of all, it is relatively long so in practical applications it is likely that it is encountered frequently and possibly more often than the steady state. Secondly, the relatively simple structure of the flow at steady state is not very sensitive to the various parameters in models of the average flow evaluation. The void fraction distribution does, for example, only depend on the sign of the bubble lift coefficient but not its magnitude. To understand how bubbly flow evolves toward a steady state we have conducted several simulations, starting with bubbles placed randomly in a parabolic laminar velocity field. The evolution toward steady state is highly non-monotonic. First, all the bubbles migrate towards the walls leaving the center region nearly free of bubbles. Then the presence of the bubbles near the wall increases the shear there and reduces the bulk flow rate. As the flow rate is reduced, some of the bubbles migrate back into the core region until the mixture there is in hydrostatic equilibrium. The initial migration of the bubbles to the walls takes place relatively fast, but the slowing down of the liquid flow and the migration of the bubbles back into the core is a much slower process. In those simulations we do not allow the bubbles to coalesce, but if they could then the migration to the wall might promote the formation of either larger bubbles that would move away from the wall relatively quickly or possibly a gas film at the wall. We have done a few simulations with a range of governing parameters and different initial bubble locations and confirmed that the overall evolution is similar in all cases and that the time scale is also comparable. However, unlike the statistically steady state, where the flow structure is relatively simple and in some cases depends only on the sign of the lift coefficient, the transient evolution is more sensitive to the governing parameters.

3.2 Closure by Statistical Learning

To explore how to use DNS results to provide closure terms for equations for the average flow, we have examined the use of Neural Networks (NN) to fit the data from the DNS. The flows that have considered so far consist of several nearly spherical bubbles rising in periodic domains with no walls, where the initial vertical velocity and the average bubble density is homogeneous in two directions but not in one of the horizontal directions. After an initial transient motion the average void fraction and the vertical velocity become approximately uniform. The NN is trained on a dataset from one simulation and then used to simulate the evolution of other initial conditions. The initial average velocity and void fraction depend only on the x coordinate, and not on y or z . As the flow evolves, the various averaged quantities are therefore functions of x only. Assuming that the gas phase has zero density and viscosity, that fluctuations in the viscous term can be neglected, and that the bubbles remain spherical, the equations for the gas volume fraction, α_g , and the average vertical velocity of the liquid, $\langle v \rangle$, are easily derived by averaging over the y and z coordinates. The result is:

$$\frac{\partial \alpha_g}{\partial t} + \frac{\partial F_g}{\partial x} = 0 \quad (1)$$

for the gas volume fraction, and

$$\begin{aligned} \frac{\partial}{\partial t} \alpha_l \langle v \rangle_l + \frac{\partial}{\partial x} \alpha_l \langle v \rangle_l \langle v \rangle_l \\ = -\frac{1}{\rho_l} \frac{dp_o}{dy} - g_y + v_l \frac{\partial}{\partial x} \left(\alpha_l \frac{\partial \langle v \rangle_l}{\partial x} \right) - \frac{\partial}{\partial x} \alpha_l \langle v' u' \rangle_l \end{aligned} \quad (2)$$

for the average vertical velocity of the liquid. Here the horizontal gas flux is $F_g = \alpha_g \langle u \rangle_g$, where $\langle u \rangle_g$ is the average horizontal velocity of the gas, α_l is the liquid volume fraction, and $\langle u'v' \rangle_l$ is the “streaming” stresses. Since $\alpha_g + \alpha_l = 1$ the first equation also gives α_l . In addition, $\alpha_g \langle u \rangle_g + \alpha_l \langle u \rangle_l = 0$, so the nonlinear term in the second equation can be written as: $\alpha_l \langle u \rangle_l \langle v \rangle_l = -\alpha_g \langle u \rangle_g \langle v \rangle_l = -F_g \langle v \rangle_l$. For these simulations we have no walls so the pressure gradient is set to $\rho_{avg} g_y$ to match the weight of the mixture. The unknown closure terms in the equations for the average flow are the gas flux and the streaming stresses. These are assumed to depend on the void fraction, the gradient of the void fraction and the gradient of the average liquid velocity, or:

$$F_g = f \left(\alpha_g, \frac{\partial \alpha_g}{\partial x}, \frac{\partial \langle v \rangle_l}{\partial x} \right); \quad \langle u'v' \rangle_l = g \left(\alpha_g, \frac{\partial \alpha_g}{\partial x}, \frac{\partial \langle v \rangle_l}{\partial x} \right) \quad (3)$$

All the quantities in these relations are obtained by averaging the DNS data, forming a large data base used to train the NN to find the relationship. The closure laws are then applied to other flows where the initial velocity and void fraction are different, but for which we also have DNS results to compare with. Overall, the average equations with the neural network closure reproduce the main aspects of the DNS results, including the generally rapid change initially as well as the level of unsteadiness remaining after the initial adjustment [15].

Neural networks are, of course, not the only statistical learning technique that we could have used and we have experimented with linear regressions, where we postulate a functional form for the relationship with coefficients that are determined from the data. Our current belief is that the neural networks are more general and require less user input. We also note that there are several versions of neural networks and related approaches and we have made no effort to find the best one. The biggest drawback of the neural network approach is that there is little physics in the fitting. This is, presumably, both strength and a weakness: On the one hand we do not need to know much about the physics to obtain the closures, but on the other hand, knowledge of the physics is of little help, at least for the approach that we have been exploring.

It is important to emphasize that the system we have examined so far are very simple one. First of all it is homogeneous in two directions so the averaged equations depend on only one spatial coordinate. Secondly, it is periodic in all directions and there are no walls; and thirdly, no average descriptions of unresolved quantities appear to be necessary (which might be governed by their own evolution equations with unknown closure terms). Furthermore the gas flux appears to a function of the local state only and no evolution equation for the bubble velocity needs to be solved. Most multiphase flows are considerably more complex than this, but we believe that there is nothing that intrinsically limits using statistical learning for the closure terms to simple systems only. We are currently exploring applications of this strategy to more complex flows, including those involving walls and bubbles of different sizes.

4. LARGE SYSTEMS

While our initial efforts to study transient bubbly flows in vertical channels have focused on relatively small systems with bubbles of only one size, there is a clear need to examine more complex systems. We are currently conducting one such run, using 2048 processors on the Titan supercomputer at ORNL. The domain size is $2\pi \times 4 \times \pi$ in the streamwise, wall-normal and spanwise direction, respectively, resolved by $1024 \times 768 \times 512$ grid points. The physical parameters are selected such that the Morton number is equal to 5.75×10^{-10} and the void fraction is 0.0304. The bubbles come in four sizes with Eo ranging from

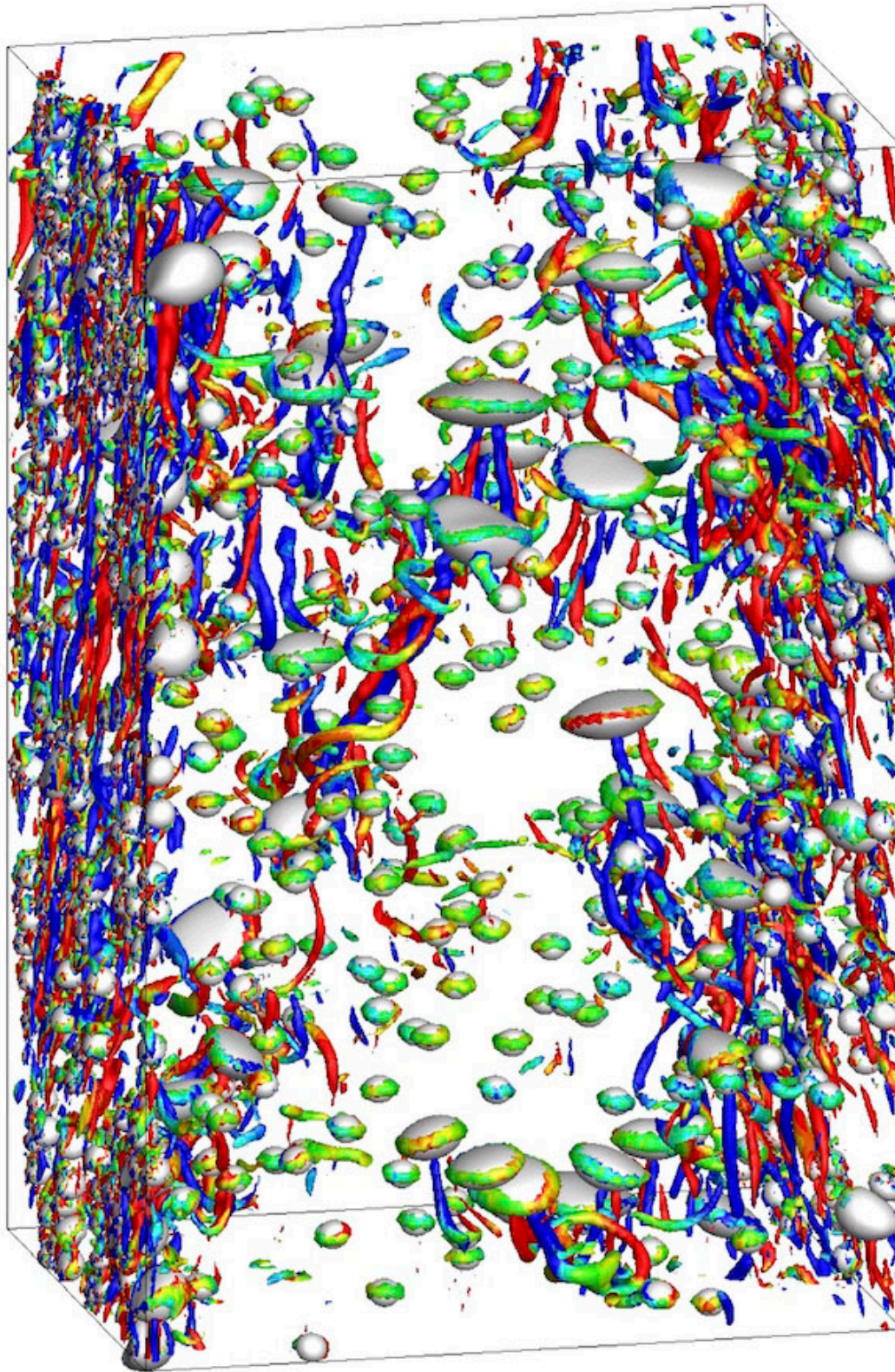


Figure 1. Bubbles and vortices visualized by the iso-surface of $\lambda_2=-2$, at time 34. Here red indicates a positive streamwise component and blue a negative one. Light blue, green and yellow are horizontal vortices.

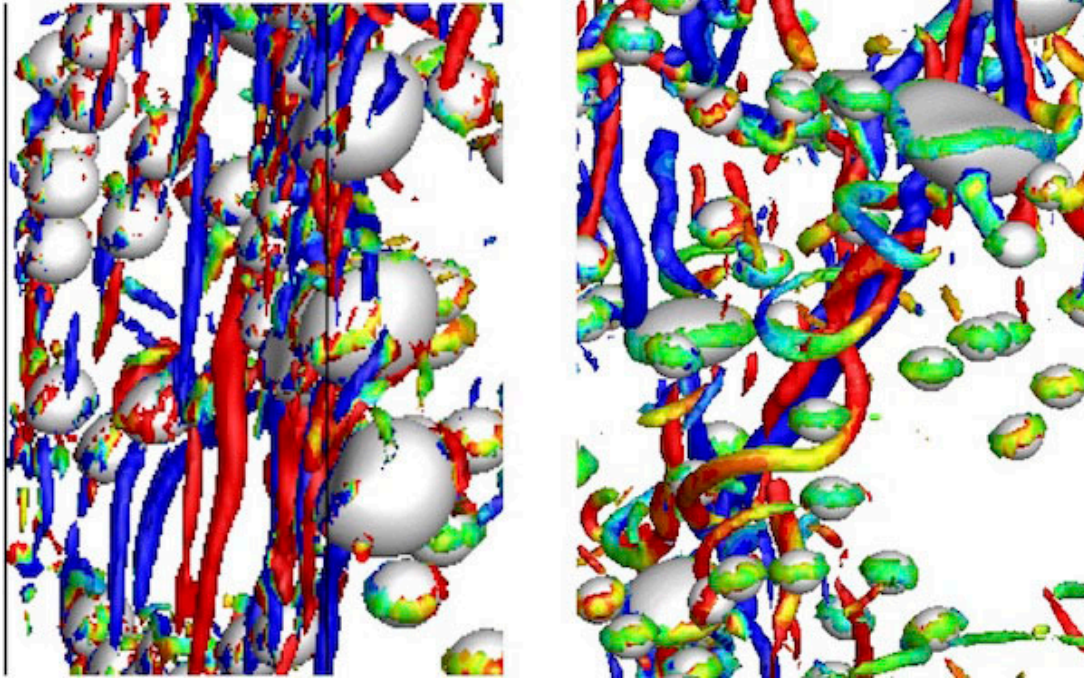


Figure 2. Close up of the vortical structures at time=64. On the left we show vorticity next to the left wall (using $\lambda_2=-2$) and on the right we show vorticity in the interior of the domain (using $\lambda_2=-4$).

0.5 to 3.8. The majority of the bubbles are small and we expect the smallest two sets of bubbles to accumulate at the wall, since our earlier results suggest that the transition between bubbles pushed to the wall and those that are not is around $Eo=2.5$. The numbers of bubbles for each group were selected so that there are enough small bubbles that can be pushed to the wall to put the core in hydrostatic equilibrium. The properties of the fluid and the bubbles are the same as in our earlier simulations, but the domain size is eight times larger, giving a friction Reynolds number of $Re^+ = 500$. The bubbles are initially distributed nearly uniformly across the domain but as they start to rise, the smaller bubbles start to migrate toward the walls and form a dense wall-layer. For channels with spherical bubbles, where the lift force pushes the bubbles toward the wall and a bubbly wall-layer is formed, it can be shown that the steady state consists of a wall-layer and a homogeneous core region where the number of bubbles is such that the weight of the mixture balances the imposed pressure gradient. Thus, if the overall void fraction is given, the void fraction in both the core and the wall-layer can be found. To understand the vortical structure, we show the bubbles and the vorticity in figure 1, visualized by the λ_2 method introduced by [16], but coloring the vortical structures according to their orientation. Thus, both red and blue vortical structures are aligned with the flow, but red have a positive rotation while the blue ones have a negative rotation. The intermediate colors (light blue, green and yellow) indicate vortical structures that are not aligned with the flow. As expected, the majority of the vortical structures aligned with the flow come in pairs, such that a blue structure is found next to a red one. We have examined the vorticity for several times, including varying the iso-contour value for λ_2 , and in figure 2 we show a close up of the vorticity for two regions of the flow at time 64. On the left we show the vorticity next to the left wall (using $\lambda_2=-2$) and on the right we look at the vorticity in the interior, now using $\lambda_2=-4$, so the vorticity appears more concentrated and low levels of vorticity are not visible. The figure shows that the longitudinal vortices, that one expects in a turbulent boundary layer, appear to survive the addition of the bubbles to the wall-layer, at least at the time plotted here, and that vorticity shed by the large bubbles is responsible for the majority of the vorticity in the interior of the channel. Vortices that are mostly horizontal do, for the most part, encircle bubbles.

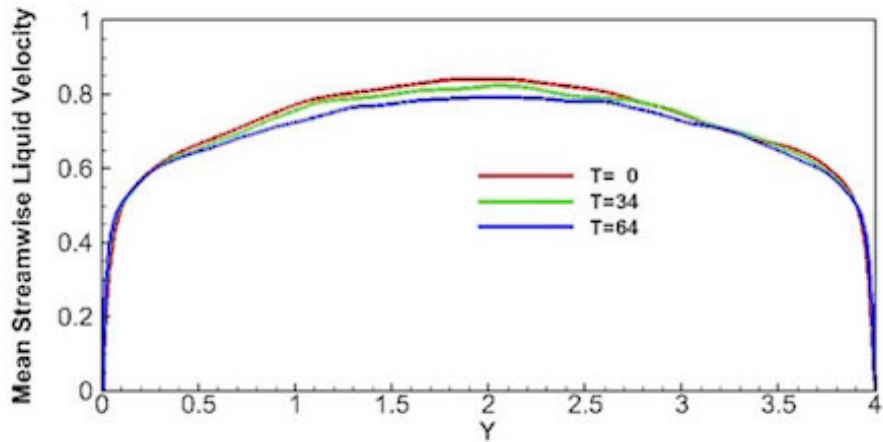


Figure 3. The mean streamwise liquid velocity across the channel at different times.

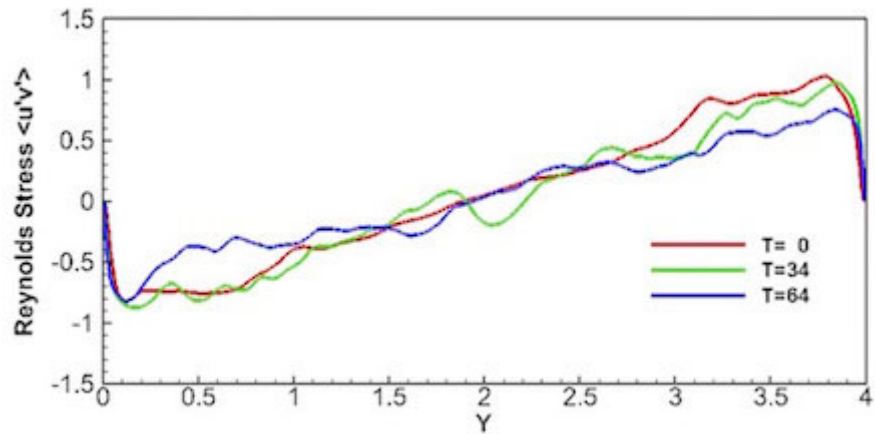


Figure 4. The Reynolds stresses (normalized by $(u^+)^2$, where u^+ is the friction velocity) across the channel at different times.

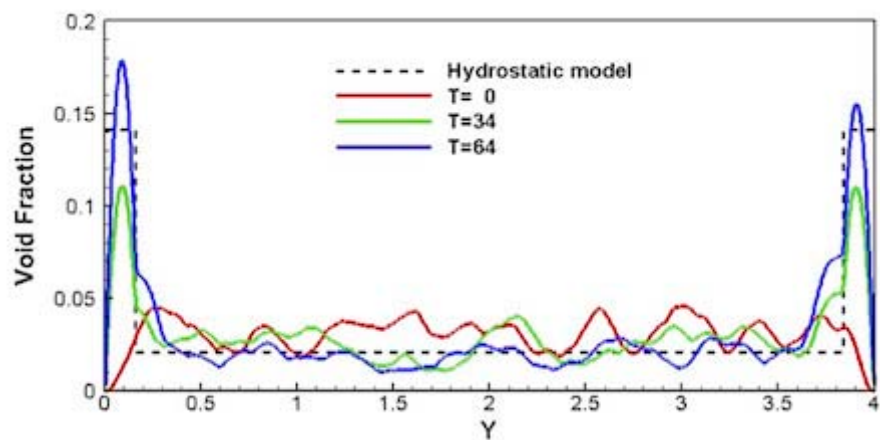


Figure 5. The void fraction at three different times, along with the predictions of a simple model for the void fraction at steady state.

In figures 3-5 we show a few quantities averaged over planes parallel to the walls, versus the horizontal coordinate at three times (4, 34, and 64, all in computational units). The average streamwise velocity is plotted in figure 3 and it is clear here that the average velocity has not changed much, so far. This is expected since the small bubbles must first move to the wall to form a layer before the presence of the layer starts to influence the velocity. As the flow evolves further, however, we expect the presence of the bubbles at the wall to reduce the flow rate. Experience with bubbles in turbulent upflow at smaller Reynolds numbers and in smaller laminar systems suggest that this will take significant time. The modest modification of the flow due to the presence of the bubbles at the early times is also seen in figure 4, where the turbulent shear, $\langle u'v' \rangle$, is plotted versus the horizontal coordinate. At steady state, $\langle u'v' \rangle$ should go to zero in the middle of the channel, if the evolution is the same as we have seen for smaller systems. The average profile has not changed much at time 34, and shows the linear shape expected for a single-phase flow, but at time 64 it has leveled off slightly, indicating that flow is starting to change. Figure 5 shows that while the average velocity has not changed much, the void fraction has. The black dashed line is the predictions of the simple model for the void fraction at steady state originally presented in our earlier work. Initially, the bubbles are relatively uniformly distributed but as they start to move upward the small bubbles start to migrate toward the wall. This leads to an increase in the void fraction there and at the latest time the distribution has almost reached the steady state value.

Similar plots of other averaged quantities show, for example, that the vorticity in the center of the channel increases slightly, as the bubbles start to move and generate vorticity, and that the structure of the vorticity near the wall starts to change. At the earliest time we see the vorticity distribution we expect for a single phase flow: a peak close to the wall corresponding to hairpin vortices and then a maximum right at the wall corresponding to the wall-bound vorticity needed to bring the velocity to zero. When the bubbles move toward the wall this changes and we see a significant increase in the vorticity near the wall. Plots of the turbulent kinetic energy show a slight increase as the bubbles start to modify the flow, both near the walls as well as in the middle of the channel, and dissipation rate increases both near the walls and in the middle of the channel.

As the void fraction distribution in figure 5 shows most clearly, the flow is evolving and given the steady state results for smaller systems and lower Reynolds numbers we expect its structure to continue to change. Indeed, plots of the flow rate of the liquid and the wall-shear stress versus time show that the system is far away from the steady state where the wall-shear balances the weight of the mixture plus the pressure gradient. The initial conditions are set up such that wall-shear balanced the weight and the pressure gradient, but as the bubbles move to the wall, they increase the wall-shear and the flow must therefore decelerate, as is seen in the liquid flow rate. Eventually the shear rate will start to decrease again and asymptotically approach the steady state value. We note, however, that some aspects, such as the average velocity, have not changed much for the time examined here. This suggests that care must be exercised when interpreting short time results for turbulent bubbly flows since the results may appear to be at steady state whereas they actually are still evolving but on a relatively long timescale. Furthermore, the results suggest that it is important to follow the evolution for a longer time to capture fully the modification that the bubbles have on the flow.

So far, we have focused on the average properties of the flow and how they evolve. Increasingly, however, as computer power increases, there is an interest in modeling multiphase flows using large eddy simulations or LES, or similar approaches where only the large-scale motion is resolved. The standard approach to LES is to filter the Navier-Stokes equations to derive equations for the large scale and we have started to use the results described above to explore the structure of the filtered fields. For other work on filtering of the Navier-Stokes equations for multiphase flows, see references [17-23].

A simple box filter is defined by:

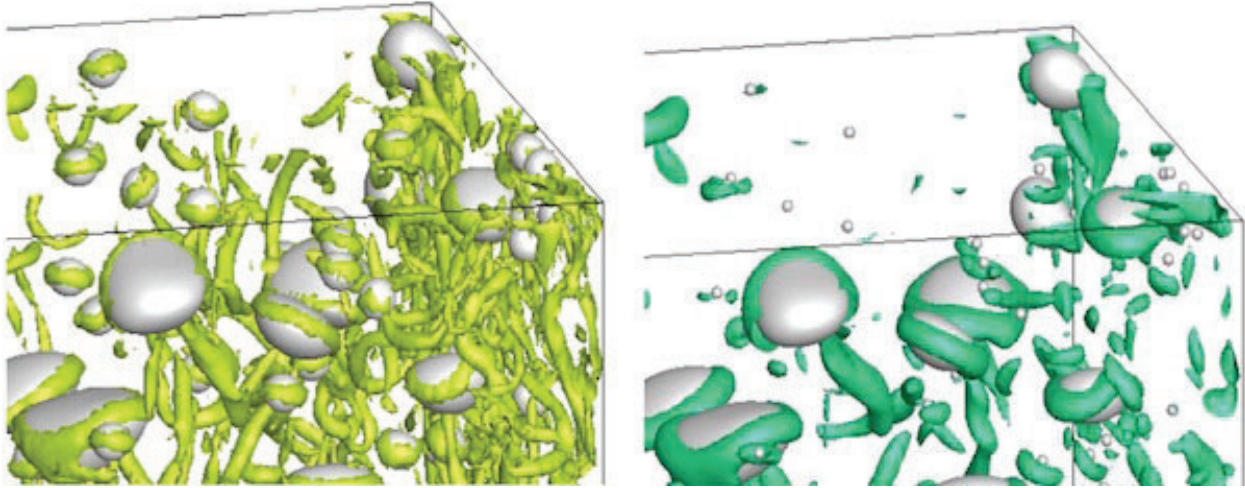


Figure 6. The original flow field and the flow field after applying a box filter that is slightly larger than the diameter of the smallest bubbles. $\lambda_2=-2$ on the left and $\lambda_2=-1$ on the right.

$$G_{\Delta}(\mathbf{x}) = \begin{cases} 1 & \text{if } |\mathbf{x}| < \Delta \\ 0 & \text{if } |\mathbf{x}| > \Delta \end{cases} \quad (4)$$

and applying it to both the velocity field and the interface results in

$$\bar{\mathbf{u}}(\mathbf{x}) = \int G_{\Delta}(\mathbf{x} - \mathbf{x}') \mathbf{u}(\mathbf{x}') d\mathbf{x} \quad \text{and} \quad \bar{\mathbf{X}}(s) = \int G_{\Delta}(\mathbf{X}(s) - \mathbf{X}(s')) \mathbf{X}(s') ds', \quad (5)$$

where the bar denotes the filtered quantity. Notice that here we apply the filter separately to the velocity field and the interface. We could, of course, also have applied the filter to the indicator function (as in [17]) but then bubbles smaller than the filter size disappear, instead of collapsing to a point particle, as happens in the present approach.

Applying the filtering to the flow field and the interface results in smoother flow. In figure 6 we show a small part of the domain at time 34, before we apply the filter (left frame) and after we apply the filter (right frame). The filter size is slightly larger than the smallest bubbles so those collapse to point particles (for plotting purpose we give them a finite size), the larger bubbles become rounder and the maximum vorticity is reduced. As noted in the figure caption, we use a different value for the iso-contours of λ_2 in the different frames to allow us to better see the vortical structures.

5. FLOWS WITH TOPOLOGY CHANGES

Although much of our work on DNS of multiphase flows has focused on bubbly flows in many cases, particularly if the void fraction is high, the interface topology is much more complex and the interfaces undergo continuous coalescence and breakup. Modeling such flows is still very primitive and we expect DNS to be able to cast considerable light on the various processes governing such flows. Topology changes in multiphase flows take place through two primary mechanisms: films that rupture and threads that break. DNS must be able to accurately handle both. For methods that track the indicator function identifying the different fluids, or phases, directly on an Eulerian grid (such as VOF or Level Set methods), topology change takes place when the resolution of a film or a thread is sufficiently low, whereas methods that use connected marker points to track the interface will generally not allow a change in topology. Both methods can be modified to either allow or prevent topology changes, but at the cost of additional coding and possibly increased runtime. Of the two types of topology changes, thin threads that break are by far the easier to deal with. The Navier-Stokes equations predict that the diameter of threads

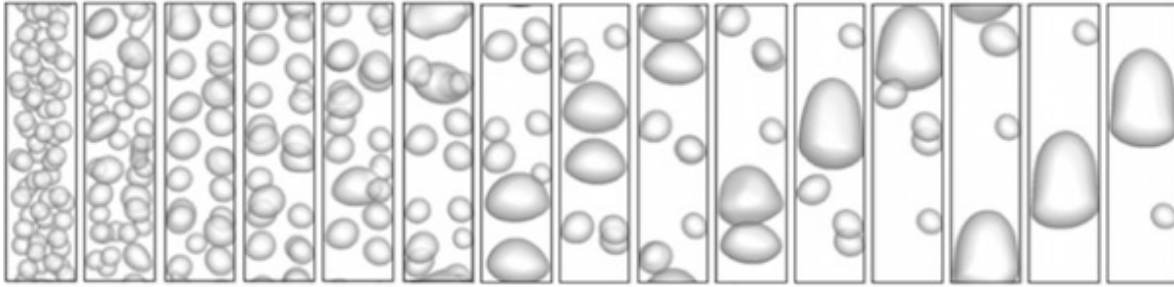


Figure 7. The transition from bubbly flow to slug flow in a vertical channel, for relatively high void fraction. Time goes from left to right.

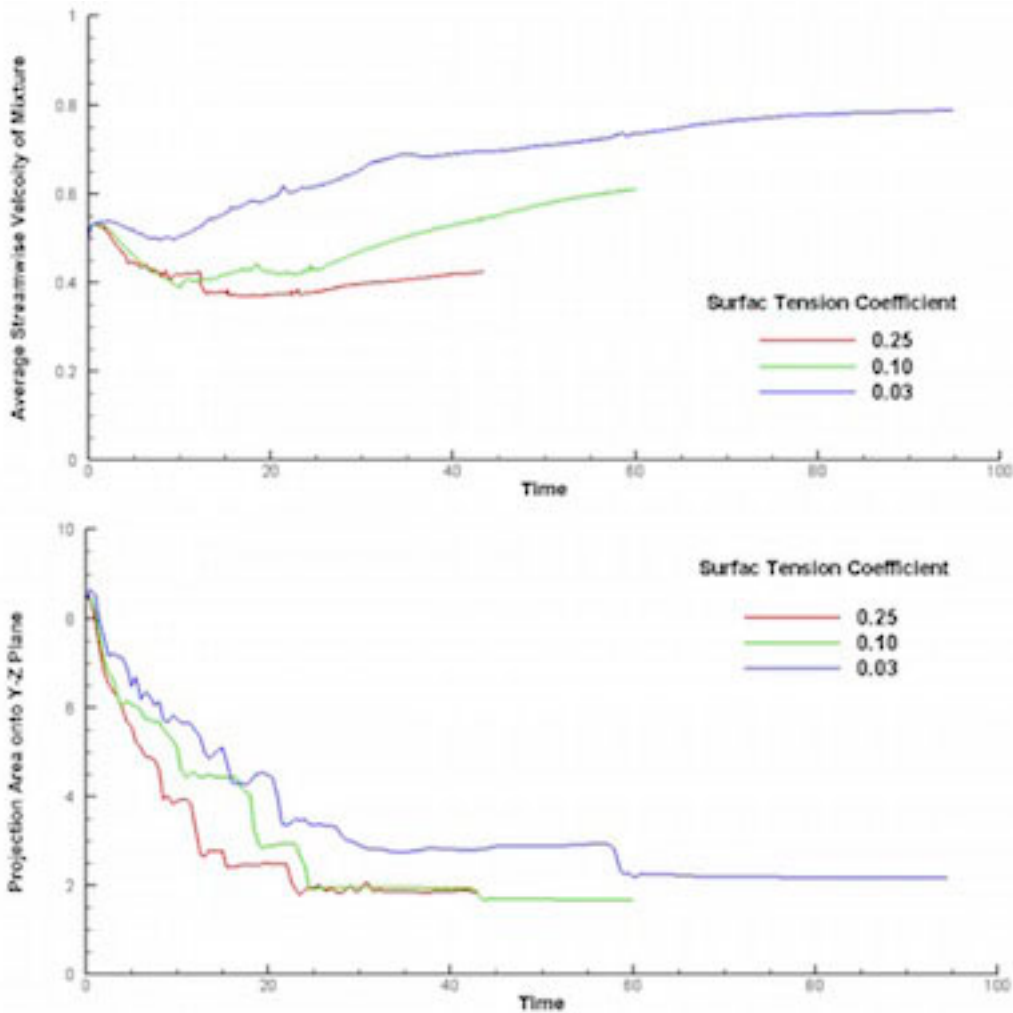


Figure 8. The average velocity of the mixture versus time for three runs with different surface tension (top) and the projection of the surface area in the streamwise direction (bottom), versus time.

becomes zero in a finite time and no additional physical modeling needs to be included. Furthermore, the breakup is fast, so while there may be a moment just before the thread breaks when it is not well resolved, this is often such a short time that it does not have a significant effect on the overall dynamics of the flow. Both types of methods generally handle thread breakup easily, with marker point methods leaving an inert

string of particles behind. The rupture of thin films is a much more complex matter. The thickness of a draining film, simulated using the standard Navier-Stokes equations, does usually not become zero in a finite time and it is only because of the presence of short range attractive forces that it eventually becomes unstable and holes are formed. The initial hole is then usually enlarged by either the formation of other holes that merge with the first one or the enlargement of the original hole by rim breakup that includes the formation of drops with threads that snap, but often on such a small scale that it is difficult to resolve them fully in simulations focusing on a larger region of the flow. The rupture of films in simulations using numerical methods that track the indicator function directly is an artifact of the finite resolution and in some cases it is found that refining the grid postpones the rupture and prevents the solution from converging to a grid independent form. While in many cases such methods produce methods that look “physical,” it is not well understood when the rupture is adequately controlled artificially by the resolution and when more complete rupture models must be included. When the interface is tracked by connected marker points it is necessary to add a strategy to rupture the interfaces when they are close enough but this results in a complete control of when, or under what circumstances, rupture takes place, thus allowing us to examine how sensitive the overall evolution of the flow is to how the rupture takes place, even if a complete rupture model is not included.

We have started to explore the dynamics of flows undergoing topology changes by doing a few simulations of the transition from bubbly flows to slug flow---so far working only with laminar flows. This transition takes place mostly through the rupture of thin films, as the bubbles coalesce, although bubble breakup and the breaking of thin threads is also seen. Our topology change algorithm seems to work well for both mechanisms, but we note that although it was developed several years ago, it has not been published yet.

Figure 7 shows results from one simulation of the coalescence of several bubbles in a channel into a large slug. The simulation is done using a grid with 320 by 80 by 80 grid points and thin films are ruptured if they become thinner than one grid spacing, thus making the results similar to what we would expect from a VOF or Level Set computation. The first frame shows the bubbles, as placed in an initially parabolic flow, and subsequent frames show the bubbles gradually becoming larger and fewer, until in the last frame we see one large slug and one small bubble. In this case the void fraction is 21% and the initial number of bubbles is sixty. The surface tension is selected such that the initial Eötvös number is 0.45.

We have explored the evolution for several different surface tension coefficients and in figure 8 we show the time evolution for three simulations with different surface tension. In the top frame the average velocity of the mixture is plotted versus time for the three runs and it is not surprising that the velocity is highest for the lowest surface tension case, where the bubbles are most compliant. In the bottom frame we show the projection of the surface area in the streamwise direction. As the bubbles coalesce, their total surface area decreases rapidly and approaches twice the cross sectional area of the channel, as we would expect for a bubble that almost fills the channel. Notice that the high surface tension bubbles coalesce most rapidly and that the simulations were terminated once all the bubbles had coalesced into one.

6. CONCLUSIONS

In addition to providing fundamental insight into the flow evolution, DNS results provide data for the unresolved closure terms in equations for the average model. We have recently started to mine the data, using various techniques such as regression and neural networks. For the average equations for simple flows the results are promising. We are also examining the use of a similar approach for LES-like simulations of more complex flows, including for a large number of bubbles of several different sizes in turbulent upflow. As the void fraction increases the assumption of bubbly flows becomes unrealistic and it is necessary to account for topological changes through coalescence and breakup and flow regime transitions. We have started to examine the transition of high void fraction bubbly flows to slug flow, and

since we use a front tracking method where the exact coalescence criteria can be changed, the details of the coalescence can be examined.

ACKNOWLEDGMENTS

This work is supported by the National Science Foundation Grant CBET-1335913 and the Consortium for Advanced Simulations of Light Water Reactors (CASL). This research used resources of the Oak Ridge Leadership Computing Facility at the Oak Ridge National Laboratory, which is supported by the Office of Science of the U.S. Department of Energy under Contract No. DE-AC05-00OR22725.

REFERENCES

- 1 A. Prosperetti and G. Tryggvason. *Computational Methods for Multiphase Flow*. Cambridge University Press, 2007.
- 2 S. O. Unverdi and G. Tryggvason, “A front-tracking method for viscous, incompressible, multi-fluid flows”, *J. Comput. Phys.* 100, 1992, 25–37.
- 3 A. Esmaeeli and G. Tryggvason, “Direct Numerical Simulations of Bubbly Flows. Part I— Low Reynolds Number Arrays.” *J. Fluid Mech.* 377 (1998), 313-345.
- 4 G. Tryggvason, B. Bunner, A. Esmaeeli, D. Juric, N. Al-Rawahi, W. Tauber, J. Han, S. Nas, and Y.-J. Jan, “A Front Tracking Method for the Computations of Multiphase Flow.” *J. Comput. Phys.* 169, 2001, 708–759.
- 5 G. Tryggvason, R. Scardovelli, and S. Zaleski, “Direct Numerical Simulations of Gas-Liquid Multiphase Flows”, Cambridge University Press, 2011.
- 6 S. Biswas, A. Esmaeeli, and G. Tryggvason, “Comparison of results from DNS of bubbly flows with a two-fluid model for two-dimensional laminar flows.” *Int’l J. Multiphase Flows*, vol. 31, pp. 1036-1048, 2005.
- 7 S.P. Antal, R.T. Lahey and J.E., Flaherty, “Analysis of phase distribution in fully developed laminar bubbly two- phase flow.” *Int. J. Multiphase Flow*, vol. 17, pp. 635–652, 1991.
- 8 J. Lu, S. Biswas, and G. Tryggvason, “A DNS study of laminar bubbly flows in a vertical channel,” *Int’l J. Multiphase Flow* 32, 2006, 643-660.
- 9 A.C. Rust and M. Manga. The effects of bubble deformation on the viscosity of suspensions, *Journal of non-Newtonian Fluid Mechanics*, vol. 104 (2002), 53-63.
- 10 B. Figueroa-Espinoza and R. Zenit. Clustering in high Re monodispersed bubbly flows. *Phys. Fluids* 17 (2005), 091701.
- 11 A. Tomiyama, H. Tamai, I. Zun, and S. Hosokawa. Transverse migration of single bubbles in simple shear flows. *Chem. Eng. Sci.* 57 (2002), 1849–1858.
- 12 A. Kariyasaki, “Behavior of a single gas bubble in a liquid flow with a linear velocity profile.” *Proceedings of the 1987 ASME-JSME Thermal Engineering Joint Conference*, edited by P.J. Marto and I. Tanasawa (ASME, New York, 1987), Vol. 5, p. 261.
- 13 E.A. Ervin and G. Tryggvason. The rise of bubbles in a vertical shear flow. *ASME J. Fluid Engineering* 119 (1997), 443-449.
- 14 K. Sankaranarayanan, X. Shan, I. G. Kevrekidis, and S. Sundaresan. Analysis of drag and virtual mass forces in bubbly suspensions using an implicit formulation of the lattice Boltzmann method. *J. Fluid Mech.* 452 (2002), 61-96.
- 15 M. Ma, J. Lu, and G. Tryggvason. Using Data Mining to Close Two-Fluid Multiphase Flow Equations for a Simple Bubbly System. Submitted for publication.
- 16 J. Jeong and F. Hussain. On the Identification of a Vortex. *J. Fluid Mechanics*, 285 (1995) 69–94.
- 17 E. Labourasse, D. Lacanette, A. Toutant, P. Lubin, S. Vincent, O. Lebaigue, J.-P. Caltagirone, P. Sagaut. Towards large eddy simulation of isothermal two-phase flows: Governing equations and a priori tests. *International Journal of Multiphase Flow* 33 (2007) 1-

- 18 A. Toutant, E. Labourasse, O. Lebaigue, and O. Simonin. DNS of the interaction between a deformable buoyant bubble and spatially decaying turbulence: a priori tests for LES two-phase flow modelling. *Comp. Fluids* 37 (7), 2008, 877-886.
- 19 S. Vincent, J. Larocque, D. Lacanette, A. Toutant, S. Lubin, and P. Sagaut. Numerical simulations of phase separation and a priori two-phase LES filtering. *Comput. Fluids* 37 (7), 2008, 898-906.
- 20 A. Toutant, M. Chandesris, D. Jamet, and O. Lebaigue. Jump conditions for filtered quantities at an under-resolved interface. Part 1: Theoretical developments. *Int. J. Multiphase Flow* 35 (12), 2009, 1100-1118.
- 21 A. Toutant, M. Chandesris, D. Jamet, and O. Lebaigue. b. Jump conditions for filtered quantities at an under-resolved interface. Part 2: A priori tests. *Int. J. Multiphase Flow* 35 (12), 2009, 1119-1129.
- 22 P. Trontin, S. Vincent, J. Estivalezes, and J. Caltagirone. Direct numerical simulation of a freely decaying turbulent interfacial flow. *International. Journal of Multiphase Flow* 36 (11—12), (2010), 891-907.
- 23 D. Jamet, O. Lebaigue, C. Morel, B. Arcen. Towards a multi-scale approach of two-phase flow modeling in the context of DNB modeling. *Nuclear Engineering and Design* 240 (2010) 2131-2138.